International Journal of Computational and Theoretical Chemistry
2018; 6(2): 28-36
http://www.sciencepublishinggroup.com/j/ijctc
doi: 10.11648/j.ijctc.20180602.11
ISSN: 2376-7286 (Print); ISSN: 2376-7308 (Online)

Effect of an External Electric Field on Structure, Stability and Energetic of $Mg^{2+}CH_3OH$ Complex: A DFT Study

Safinaz H. El-Demerdash

Chemistry Department, Faculty of Science, El-Menoufia University, Shebin El-Kom, Egypt

Email address:
hamdysafinaz@yahoo.com

To cite this article:
Safinaz H. El-Demerdash. Effect of an External Electric Field on Structure, Stability and Energetic of $Mg^{2+}CH_3OH$ Complex: A DFT Study. *International Journal of Computational and Theoretical Chemistry.* Vol. 6, No. 2, 2018, pp. 28-36. doi: 10.11648/j.ijctc.20180602.11

Received: November 25, 2018; **Accepted**: December 13, 2018; **Published**: January 10, 2019

Abstract: To understand the structural and stability of fragmentation of $Mg^{2+}CH_3OH$ Complex in gas phase under an external electric field, a quantum chemical calculation has been carried out with Density Functional Theory (DFT) at BMK/6-31+G (d). Different levels of applied electric field (0.0, 0.002, 0.004, 0.006, 0.008 and 0.01 a.u.) change the geometrical parameters as well as the energies of the complex. Variations in NPA atomic charges of the fragments for the applied fields were compared. The electric field was applied to the five major reaction channels of $Mg^{2+}CH_3OH$ complex. At zero fields, the complex is thermodynamically unstable with respect to the loss of CH_3OH^+, CH_3^+, and CH_3O^+ but thermodynamically stable toward the loss of H^+. The presence of large kinetic energy barriers for unimolecular dissociation prohibits the exothermic processes. With increases the field strength the thermodynamic stability of complex increases for all channels. The resultant dipole moment (μT) increases almost linearly with the increase of field. The complex becomes highly polarized for the higher field (0.01 a.u.) and the dipole moment becomes 14.77 D. The relationship between dissociation product and field strength is very complex due to the different responses of the reactants and transition states toward the external electric field.

Keywords: Electric Field, Stability, Magnesium Dication Complex, Unimolecular, Kinetics, BMK

1. Introduction

The quick development of laser techniques opens a new area for understanding the interactions of molecules with the laser field [1]. The laser field, especially the strong laser field, within the molecule can stimulate different reactions, such as multiple ionization [2], field ionization [3], and field dissociation [4, 5] and even Coulomb explosion [6, 7]. To add to this, the preferred and selectivity of bond activation in molecules and clusters can be changed due to the effect of an external electric field [8, 9]. Recently the influence of external electric field on the fragmentation of some polyatomic molecules with single or multiply charges has also been investigated theoretically [10-12], but they focused only on the individual interaction with the electric field in the fixed direction. The direction of a molecule under an electric field should be adapted according to the direction of its dipole moment. With or without an intense laser, the number of fragmentation channels for an active precursor is usually more than one and depends on its nature and energy of its fragmentation. In order to characterize the full effect of the external electric field on fragmentation of an energetic precursor, one should study the net reaction as a whole since many reaction channels can be accelerated or blocked as the field strength differs.

The electric field created by charger [13, 14] or external electric field was used to determine the hydrogen bond [15, 16]. Electric field, pressure, temperature, and density cause variation of the distance and the hydrogen bond strength [17]. The weakening or strengthening of the hydrogen bond can be explained regarding a high polarizability of the molecular orbital with the direction of the electric field applied [18].

Yamanouchi and co-workers have examined the fragmentation of methanol by intense 800 nm laser pulses, with an aim to understanding the behavior of methanol mono- and dications in strong laser fields [19−26]. Electrical field effects on dipole moment, structure and energetic of $(H_2O)_n$ ($2 < n < 15$) cluster has been studied by Rogério Custodio *et. al.* [27]. Behavior of water dimer under influence of external electric field and its ionization also have been studied theoretically [28, 29]. Theoretical study on the fragmentation of ethanol cation under an electric field has been studied by

Hsiu-Feng Lu *et.al.* [30].

Many computational and theoretical studies on chemical properties of several organic molecules have been reported and investigated using quantum theory of atoms in molecules [31, 32]. Quantum chemical calculations, Density functional theory (DFT)) method which includes optimization, are used to predict structural and electronic properties of molecules. It is used to find minima on the potential energy surface of a molecule. Optimization to minima also known as energy minimization decreases the energy of a molecule by adjusting atomic coordinates [33]. Obtaining a structure for calculating a single-point quantum mechanical gives a broad point of structural and electronic properties [33, 34]. Even though many physical and chemical phenomena are experimentally studied in condensed phases, the great majority of quantum chemical calculations for studying of the structure, properties and spectroscopy deal with isolated molecules. The current study uses quantum chemical calculations to report the structural, energetic features and their relative stability in the gas phase of $Mg^{2+}CH_3OH$ complex fragmentations under various applied electric fields.

2. Computational Details

The effect of electric field (EF) on the structural, stability and energetic of fragmentation of $Mg^{2+}CH_3OH$ Complex, has been obtained by optimizing it for the zero and applied fields [five biasing steps 0.0002 to 0.01 a.u.] for C-O and O-Mg directions. All calculations have been carried out with density functional theory (DFT) [35, 36] using Gaussian09 program [37]. All geometry optimizations were performed using density functional theory DFT/BMK as introduced by Boese and Martin [38]. For different stationary point, we carried out vibrational frequency calculations to characterize their nature as minima or transition states and to correct energies for zero-point energy. The transition states for unimolecular dissociation channels have been located using the synchronous transit-guided quasi-Newton (TS) technique, the eigenvalue-following (EF) optimization procedures as implemented in the Gaussian program [37]. The vibrational modes were examined with the Chemcraft program V1.8 [39]. Partial charge distributions were calculated using the natural population analysis (NPA) method [40]. The nature of the transition states was confirmed by the presence of one imaginary frequency in the Hessians. The BMK [38] functional gives a better performance in reproducing barrier heights for different reactions and it is use it in this work.

3. Results and Discussion

The geometrical parameters are important for adjusting the electrical properties of a molecule. Therefore, we study the change of bond length and bond angle under the electric field interaction. It is useful to understand the relationship between molecular structure and its properties.

The $Mg^{2+}CH_3OH$ produce different products under applied electric field via simple bond fission or hydrogen transfer with breaking and forming bonds (complex dissociation). Transition states for channels were located and frequency analysis confirmed these transition states. It may be susto a variety of dissociation channels which can be summarized as follows:

1. $Mg^{2+}CH_3OH \rightarrow Mg^{2+} + CH_3OH$
2. $Mg^{2+}CH_3OH \rightarrow Mg^{+} + CH_3OH^{+}$
3. $Mg^{2+}CH_3OH \rightarrow MgOH^{+} + CH_3^{+}$
4. $Mg^{2+}CH_3OH \rightarrow MgH^{+} + CH_3O^{+}$
5. $Mg^{2+}CH_3OH \rightarrow MgOCH_3^{+} + H^{+}$

3.1. Structural Properties

The optimized geometry of the CH_3OH, CH_3OH^{+}, $Mg^{2+}CH_3OH$ and transition states for different dissociations for the zero and the various applied EFs (0 -0. 01 a.u.) is illustrated in Figure 1.

In Table 1, important geometrical parameters of these species were tabulated to describe the structural changes due to the electric field.

I found that for the zero fields, the C−O bond distance of CH_3OH are 1.411 Å. When the field applied, these distances are increased slightly; however, the EF's dependence on the evaluation bond length is not the same for all the bonds; the minimum and maximum observed variation in C−O bonds are 0.003 and 0.015 Å, respectively (Table 1). In addition, the C-H bond distances under applied electric field are slightly decreased. The zero field distance of O−H bond is ~ 0.964 Å, which remains almost the same value for the increase of field. The bond angles are different under effect of EF such as O1C2H3, O1C2H4, O1C2H5 and O1C2H6 angles are deceased with increased the electric field. Almost all the bond distances and bond angles have been varied by the application of external field. My computed geometrical parameters for methanol at zero field are in good agreement with the values calculated [41, 42] at the MP2/6- 311 + G (2d, p), QCISD/6-31G (d) and B3LYP/6-311G (d, p) levels of theory. These geometrical parameters are very close to the previously reported experimental as well as theoretical values [43].

For CH_3OH^{+}, I found that the C−O bond distance does not change significantly as the field strength increases. While the C-H bond lengths under applied field are slightly increased. For example, these C2–H3 and C2-H4 bond lengths are 1.131 Å without field and become 1.140 Å with a 0.01 a.u. electric field. However, O-H bond length is slightly decreased as the field increases. The O1C2H3, O1C2H4 and O1C2H5 angles are enlarged with increased EF but O1C2H6 angle is decreased. Our calculations for geometrical parameters of CH_3OH^{+} are in good agreement with the value calculated at B3LYP/6-311G (d, p) [42].

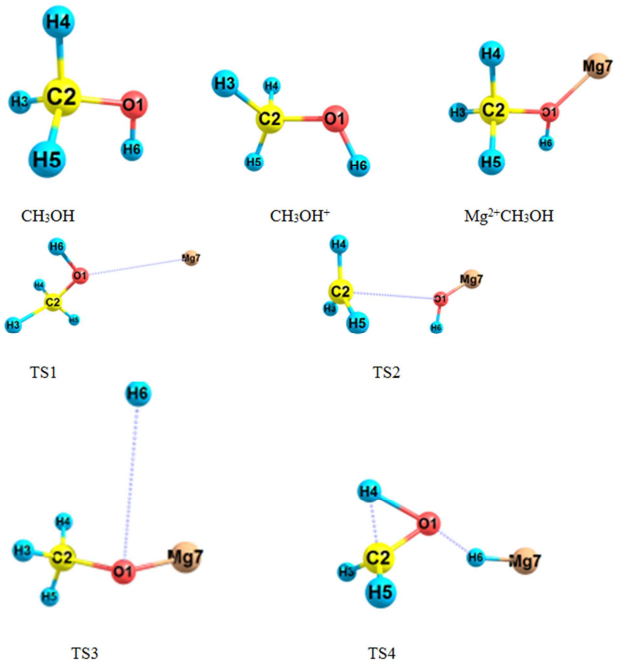

Figure 1. *Optimized structures of CH_3OH, CH_3OH^+, $Mg^{2+}CH_3OH$ and transition states for dissociation.*

Table 1 shows that the C–O bond length in complex decreases as the field strength increases. For example, this C–O bond length is 1.513 Å without field and becomes 1.497 Å with a 0.01 a.u. electric field. While the C-H bond lengths under applied field are slightly shorten. The O-H bond distance is slightly increased with increased the field. A variation has been noticed in bond angles of the complex (ca. 1-18°.). My Computed results for $Mg^{+2}CH_3OH$ complex is agree with the geometries that calculated at B3LYP/6-311G (d, p) [42].

In the transition states, a total charge of +2 e is imposed on the whole system. Therefore, we could differentiate between loss of charged and neutral species from charge distribution over the separated fragments in the transition states. The loss of Mg^+, CH_3^+ H^+ and CH_3O^+ passes through TS1-4.

As can be seen from Figure 1, a significant elongation in the breaking bonds in the relevant transition states, e.g. 4.801 Å for the Mg–O bond in TS1 compared to $Mg^{2+}CH_3OH$ at zero field. With increasing the electric field the Mg-O bond length is decreasing. The C-O bond in TS2 and O-H bond in TS3 they have the same trend of TS1 with increasing the field. In TS4 the O-Mg bond length increases with increase the field strength while C2-H4 bond length decreases with increases field strength due to the breaking bonds in the relevant transition states.

The sum of NPA charges over CH_3 fragment in TS2 of +1.1 e indicates the separation of methyl cation. In TS4, the NPA charges over the H fragment of +0.6 e reveal formation of a proton. The formation of CH_2OH cation was realized from the charge of 0.7 e over this fragment in TS3. The influence of electric field on the transition states bond lengths and bond angles (TS1-4) are noticed (Table 1). In general, the results in Table 1 show that there is large structural change for every species. However, the magnitude of these structural changes is not related to their energy decreasing when they are under an electric field. It points that the electric field affects the electronic structures of the reactants and transition states quite differently by distorting their structures in slightly different way to adjust the external electric field.

Table 1. *Geometrical parameters for CH3OH, CH_3OH^+ and $Mg^{2+}CH_3OH$ for the zero and various applied EFs (a.u.) at BMK/6-31+(d).*

Applied electric field						
parameters	**0.0**	**0.002**	**0.004**	**0.006**	**0.008**	**0.01**
CH_3OH						
C2-O1	1.411	1.414	1.417	1.419	1.423	1.426
C2-H3	1.102	1.101	1.100	1.010	1.099	1.099
C2-H4	1.095	1.094	1.094	1.094	1.094	1.093
C2-H5	1.102	1.102	1.100	1.010	1.010	1.099
O1-H6	0.964	0.964	0.964	0.963	0.963	0.963
A (O1-C2-H3)	112.0	111.9	111.8	111.7	111.6	111.6
A (O1-C2-H4)	106.6	106.7	106.7	106.8	106.7	106.7
A (O1-C2-H5)	112.0	112.0	111.9	111.8	111.6	111.6
A (H6-O1-C2)	109.5	109.1	108.6	108.3	107.9	107.5
CH_3OH^+						
C2-O1	1.348	1.348	1.348	1.348	1.348	1.348
C2-H3	1.131	1.133	1.135	1.137	1.139	1.140
C2-H4	1.132	1.133	1.135	1.137	1.138	1.140
C2-H5	1.092	1.092	1.092	1.092	1.093	1.093
O1-H6	0.989	0.988	0.987	0.986	0.985	0.984
A (O1-C2-H3)	106.2	106.4	106.7	107.0	107.3	107.6
A (O1-C2-H4)	106.2	106.5	106.8	107.0	107.3	107.6
A (O1-C2-H5)	116.6	116.8	117.0	117.1	117.3	117.4
A (H6-O1-C2)	115.5	114.9	114.3	113.7	113.2	112.6
CH_3OHMg^{+2}						
C2-O1	1.513	1.512	1.508	1.504	1.500	1.497
C2-H3	1.092	1.092	1.092	1.092	1.092	1.092
C2-H4	1.092	1.093	1.093	1.094	1.094	1.095
C2-H5	1.092	1.093	1.093	1.094	1.095	1.095
O1-H6	0.977	1.093	0.974	0.973	0.972	0.972
O1-Mg	1.903	1.917	1.928	1.944	1.970	1.993

Applied electric field						
parameters	**0.0**	**0.002**	**0.004**	**0.006**	**0.008**	**0.01**
A (O1-C2-H3)	107.1	107.2	107.4	107.7	107.8	108.0
A (O1-C2-H4)	106.8	107.4	107.2	107.2	106.9	106.8
A (O1-C2-H5)	107.1	107.4	108.0	108.4	109.0	109.4
A (H6-O1-C2)	107.4	109.9	111.0	111.8	112.0	112.0
A (Mg-O1-H6)	122.6	125.3	127.8	129.4	129.2	128.5
A (Mg-O1-C2)	130.1	124.9	120.7	117.5	114.6	111.7

Table 2. *Geometrical parameters for the transition states of $Mg^{2+}CH_3OH$ for the zero and various applied EFs (a.u.) at BMK/6-31+(d).*

Applied electric field						
parameters	**0.0**	**0.002**	**0.004**	**0.006**	**0.008**	**0.01**
CH_3OH^++Mg^+ (TS1)						
C2-O1	1.399	1.418	1.372	1.391	1.407	1.423
C2-H3	1.111	1.094	1.129	1.127	1.124	1.122
C2-H4	1.091	1.101	1.107	1.107	1.107	1.107
C2-H5	1.112	1.100	1.157	1.144	1.137	1.131
O1-H6	0.973	0.967	0.973	0.973	0.973	0.973
O1-Mg	4.801	4.704	2.981	2.782	2.650	2.543
A (O1-C2-H3)	111.2	107.6	108.8	108.9	108.9	108.9
A (O1-C2-H4)	108.5	111.0	117.7	117.0	116.2	115.5
A (O1-C2-H5)	110.3	111.6	113.5	114.2	114.6	114.8
A (H6-O1-C2)	109.6	109.8	112.8	112.3	111.9	111.3
A (Mg-O1-H6)	115.0	142.0	146.5	147.2	145.0	142.6
A (Mg-O1-C2)	132.8	107.7	49.0	54.0	56.9	59.1
CH_3^++ $MgOH^+$ (TS2)						
C2-O1	3.557	3.292	3.1026	2.949	2.821	2.713
C2-H3	1.094	1.093	1.093	1.092	1.091	1.091
C2-H4	1.093	1.093	1.092	1.092	1.091	1.094
C2-H5	1.094	1.093	1.093	1.093	1.093	1.091
O1-H6	0.973	0.973	0.972	0.972	0.972	0.973
O1-Mg	1.820	1.814	1.808	1.803	1.804	1.812
A (O1-C2-H3)	88.0	88.3	88.1	93.2	92.9	94.6
A (O1-C2-H4)	95.2	95.7	95.5	89.8	91.9	90.5
A (O1-C2-H5)	88.0	88.1	89.5	91.1	91.0	92.8
A (H6-O1-C2)	88.9	93.9	99.4	104.4	105.6	102.4
A (Mg-O1-H6)	118.7	121.0	124.7	129.4	133.0	132.8
A (Mg-O1-C2)	152.5	145.1	135.9	126.2	114.8	103.0
H^++CH_3OMg^+ (TS3)						
C2-O1	1.398	1.411	1.400	1.405	1.408	1.411
C2-H3	1.109	1.102	1.103	1.102	1.101	1.101
C2-H4	1.112	1.115	1.115	1.115	1.115	1.114
C2-H5	1.094	1.093	1.095	1.096	1.096	1.097
O1-H6	3.525	3.415	3.541	3.510	3.456	3.407
O1-Mg	1.826	1.868	1.843	1.865	1.882	1.900
A (O1-C2-H3)	111.4	112.7	112.8	113.5	114.0	114.4
A (O1-C2-H4)	110.5	109.1	109.4	108.9	108.5	108.2
A (O1-C2-H5)	110.2	109.4	109.9	109.7	109.6	109.7
A (H6-O1-C2)	90.2	95.9	91.0	91.5	92.0	92.7
A (Mg-O1-H6)	122.4	117.9	113.3	106.2	100.4	95.5
A (Mg-O1-C2)	137.8	133.2	132.2	127.1	123.2	119.2
CH_2OH^++MgH^+ (TS4)						
C2-O1	1.312	1.311	1.310	1.309	1.309	1.308
C2-H3	1.100	1.099	1.099	1.099	1.099	1.101
C2-H4	1.264	1.262	1.258	1.251	1.251	1.216
C2-H5	1.100	1.100	1.100	1.101	1.101	1.101
O1-H6	1.540	1.579	1.619	1.667	1.101	1.858
O1-Mg	3.227	3.248	3.295	3.392	3.392	3.686
A (O1-C2-H3)	118.6	118.8	119.0	119.2	119.2	119.0
A (O1-C2-H4)	67.5	67.7	68.4	69.6	69.6	77.9
A (O1-C2-H5)	118.6	118.3	118.0	117.8	117.8	117.0
A (H6-O1-C2)	119.5	119.2	118.5	116.8	116.8	111.7
A (Mg-O1-H6)	13.0	14.8	15.4	14.6	14.6	11.1
A (Mg-O1-C2)	132.6	128.7	123.5	118.4	118.4	110.0

3.2. Atomic Charges and Dipole Moments

To determine the atomic charges, different methods are available, the most commonly used are Natural population analysis, Mulliken population analysis and Chelpg scheme. In the current study the charges have been calculated by NPA method [40]. For the zero fields, the NPA charge for O-atom of all species is found almost negative except CH_3OH^+ and with increasing the field it gain more negative charge except complex. The H-atoms are positive except H6 in TS4. For all species the NPA charge on C atoms are negative except at TS2. When the field increases, the charges of the C atom are found almost increases except in TS2. The NPA charges of all H-atoms are decreases except H6 as the field increases. The complete values of NPA charge distribution for zero and various applied EFs are presented in Tables 3 and 4. On the whole, it is found that the all atom of species exhibit systematic variation for the increase of field. This indicates that the CH_3OH molecule is polarized by Mg^{2+} dication.

The dipole moments of the studied Complex and their dissociation channels in the gas-phase calculated at the BMK level of theory are given in Table 3. Increases in dipole moments are observed with increased field. However, the values of the increments vary according to the values of electric field in the gas-phase. The applied EF leads to redistribution of charges of the molecular chain, and therefore the dipole moment of the molecule changes [44, 45]. Thus, we can estimate the electron transport ability simply by comparing the dipole moments of the molecule to the different applied EFs. The variations of dipole moment for the various applied EF were analyzed by several researchers [46] and found a linear character. Here, I have calculated the dipole moment of the molecule for zero as well as different applied EFs. The resultant molecular dipole moment (μT) increases almost linearly with the increase of field. The complex becomes highly polarized for the higher field (0.01) a.u and the dipole moment becomes 14.77D.

Table 3. *NPA atomic charges (e) for CH_3OH, CH_3OH^+ and the $Mg^{2+}CH_3OH$ for the zero and various applied EFs (a.u.) at BMK/6-31+ (d).*

Applied electric field						
Atom	**0.0**	**0.002**	**0.004**	**0.006**	**0.008**	**0.01**
CH_3OH						
O1	-0.790	-0.793	-0.796	-0.800	-0.803	-0.806
C2	-0.334	-0.337	-0.339	-0.341	-0.343	-0.345
H3	0.200	0.202	0.205	0.208	0.211	0.213
H4	0.228	0.230	0.231	0.233	0.235	0.237
H5	0.200	0.202	0.205	0.208	0.211	0.213
H6	0.497	0.495	0.493	0.491	0.490	0.487
CH_3OH^+						
O1	0.183	0.169	0.156	0.142	0.129	0.114
C2	-0.119	-0.113	-0.107	-0.100	-0.093	-0.086
H3	0.253	0.257	0.261	0.264	0.268	0.271
H4	0.253	0.257	0.260	0.263	0.267	0.270
H5	0.146	0.148	0.149	0.150	0.152	0.153
H6	0.283	0.282	0.281	0.280	0.279	0.277
CH_3OHMg^{+2}						
O1	-1.040	-1.035	-1.028	-1.020	-1.008	-0.996
C2	-0.347	-0.361	-0.368	-0.373	-0.378	-0.384
H3	0.291	0.295	0.294	0.292	0.289	0.287
H4	0.252	0.273	0.270	0.271	0.272	0.271
H5	0.291	0.273	0.275	0.275	0.274	0.273
H6	0.602	0.604	0.603	0.601	0.597	0.593
Mg	1.951	1.952	1.953	1.954	1.954	1.955

Table 4. *NPA atomic charges (e) for transition states of $Mg^{2+}CH_3OH$ for the zero and various applied EFs (a.u.) at BMK/6-31+G (d, p).*

Applied electric field						
Atom	**0.0**	**0.002**	**0.004**	**0.006**	**0.008**	**0.01**
CH_3OH^++Mg^+ (TS1)						
O1	-0.621	-0.775	-0.766	-0.790	-0.803	-0.815
C2	-0.355	-0.345	-0.476	-0.532	-0.568	-0.594
H3	0.283	0.208	0.220	0.236	0.252	0.264
H4	0.258	0.247	0.381	0.392	0.399	0.405
H5	0.294	0.242	0.147	0.187	0.211	0.231
H6	0.538	0.530	0.573	0.575	0.576	0.577
Mg	1.602	1.893	1.921	1.930	1.932	1.931
CH_3^++ $MgOH^+$ (TS2)						
O1	-1.406	-1.410	-1.413	-1.416	-1.414	-1.406
C2	0.199	0.190	0.181	0.167	0.140	0.111
H3	0.262	0.264	0.267	0.271	0.279	0.286
H4	0.262	0.261	0.260	0.259	0.266	0.255
H5	0.263	0.263	0.263	0.263	0.256	0.268

Applied electric field						
Atom	**0.0**	**0.002**	**0.004**	**0.006**	**0.008**	**0.01**
H6	0.528	0.536	0.544	0.553	0.562	0.569
Mg	1.892	1.896	1.899	1.904	1.911	1.916
H^++CH_3OMg^+(TS3)						
O1	-1.147	-0.984	-0.968	-0.952	-0.941	-0.927
C2	-0.337	-0.356	-0.365	-0.373	-0.380	-0.387
H3	0.329	0.279	0.263	0.256	0.253	0.249
H4	0.329	0.279	0.287	0.288	0.286	0.285
H5	0.319	0.255	0.262	0.266	0.267	0.268
H6	0.561	0.609	0.607	0.604	0.604	0.601
Mg	1.946	1.918	1.914	1.912	1.911	1.910
CH_2OH^++MgH^+ (TS4)						
O1	-0.386	-0.369	-0.347	-0.316	-0.269	-0.199
C2	-0.094	-0.097	-0.105	-0.120	-0.156	-0.220
H3	0.293	0.292	0.292	0.293	0.295	0.304
H4	0.520	0.517	0.512	0.504	0.492	0.476
H5	0.293	0.291	0.288	0.284	0.280	0.275
H6	-0.355	-0.369	-0.380	-0.389	-0.398	-0.403
Mg	1.729	1.734	1.740	1.745	1.755	1.767

Table 5. *Dipole moments (Debye) for CH_3OH, CH_3OH^+, $Mg^{2+}CH_3OH$ and transition states for the zero and various applied EFs (a.u.) at BMK/6-31+G (d, p).*

Species	**DM**					
	0.0	**0.002**	**0.004**	**0.006**	**0.008**	**0.01**
CH_3OH	2.006	2.0223	2. 0784	2.1368	2.1975	2.2601
CH_3OH^+	1.822	4.717	4.8231	4.9298	5.0372	5.1453
$Mg^{+2}CH_3OH$	8.839	12.784	12.8232	12.8629	12.9028	14.7650
TS1	19.829	32.432	32.3782	24.5592	22.9026	22.9876
TS2	5.051	12.072	12.1496	12.2210	12.2887	12.3542
TS3	9.035	9.180	14.0620	14.2093	14.3564	14.5035
TS4	11.877	18.542	20.0897	18.6194	18.6558	18.6906

3.3. Energies

The energetic for the fragmentation of $Mg^{+2}CH_3OH$ is summarized in Figure 2 and in Table 6. The energy barrier of any given reaction must change when the energetic precursors are under an electric field as compared to the absence of field, mainly due to different responses to the electric field between the reactant and TS. The behavior of overall reaction is also because the responses to the electric field between different interaction channels. We applied the electric field to the five channels with five different electric dipole field strengths, 0, 0.002, 0.004, 0.006, 0.008 and 0.01 atomic units (a.u.)

Table 6. *Zero-point corrected relative energies (RE, kcal/mol) for CH_3OH, CH_3OH^+, $Mg^{2+}CH_3OH$ and transition states for the zero and various applied EFs (a.u.) at BMK/6-31+G (d, p).*

Species	**RE BMK/6-31+G (d, p)**					
	0.0	**0.002**	**0.004**	**0.006**	**0.008**	**0.01**
CH_3OH^++Mg^+	-12.05	-9.23	-5.80	-2.12	1.53	5.35
CH_3^++$MgOH^+$	-9.07	-8.20	-8.17	-7.72	-7.69	-7.59
CH_3O^++MgH^+	-27.41	-19.53	-11.00	-2.30	6.31	15.06
H^++CH_3MgO^+	98.56	109.28	119.69	125.93	129.51	136.30
$Mg^{+2}CH_3OH$	0.0	0.0	0.0	0.0	0.0	0.0
TS1	69.14	58.77	39.58	38.11	36.89	36.76
TS2	38.96	42.44	46.37	50.71	54.38	57.95
TS3	121.08	134.94	136.96	137.90	137.92	137.55
TS4	109.14	111.12	110.89	108.93	106.06	101.61

All energies were corrected for ZPEs. Binding energies (BEs) were calculated by subtracting total energies of Mg^{2+} andCH_3OH from those of $Mg^{2+}CH_3OH$. The energy difference between the transition state and the corresponding $Mg^{2+}CH_3OH$ complex defines the energy barrier of the respective dissociation process.

The results shown in figure 2 indicate that channel 5 is energy demanding process (highly endothermic) and unlikely occur except when higher temperature is provided to the reaction system. On the other hand, channels 2, 3 and 4 are exothermic where the dissociation products are thermodynamically stable with respect to the dication complex. This indicates that unimolecular dissociation paths 2, 3 and 4 can occur spontaneously unless sufficient kinetic energy barriers exist to hinder such transformation

As shown in Figure 2 at zero fields, $Mg^{2+}CH_3OH$ is thermodynamically and kinetically stable toward dissociation to H^+ with increasing the electric field, the thermodynamic

stability increases and is not preferable kinetically. On the other hand, at zero fields, $Mg^{2+}CH_3OH$ is thermodynamically unstable toward $Mg^{+}+CH_3OH^{+}$ and CH_3O^{+} but kinetically favored. With increasing electric field, they become thermodynamically and kinetically more stable. With increasing the field strength the CH_3^{+} formation is kinetically prohibited but it is favorable thermodynamically. We conclude that the stability of complex increases with increases electric field for all channels. The complex is thermodynamic stable for the loss of Mg^{+}, CH_3^{+} and CH_3O^{+} with additional kinetic stabilization based on the existence of energy barriers (see table 6 and figure 2). Loss of proton from $Mg^{2+}CH_3OH$ through energy barriers of 121-137 kcal/mol for different electric field means that dissociation processes can occur unless high temperature of the reaction system is provided. The reaction shows high endothermicity indicating kinetically and thermodynamically stable complex. Formation of magnesium cation needs 37-69 kcal/mol as the field increases, while the production of CH_3O^{+} and methyl cation (CH_3^{+}) require 102-109 and 39-58 kcal/mol, respectively with the field increases. Based only on this thermodynamic behavior, one cannot expect the presence of $Mg^{2+}CH_3OH$ experimentally because it will dissociate spontaneously to monopositive fragments. However, the presence of large energy barriers prohibits this molecular dissociation and the $Mg^{2+}CH_3OH$ complex can be observed experimentally. My calculated energies at zero fields are very good with value that calculated at B3lyp/6-31+G (d, p) and CBS-QB3 levels [42].

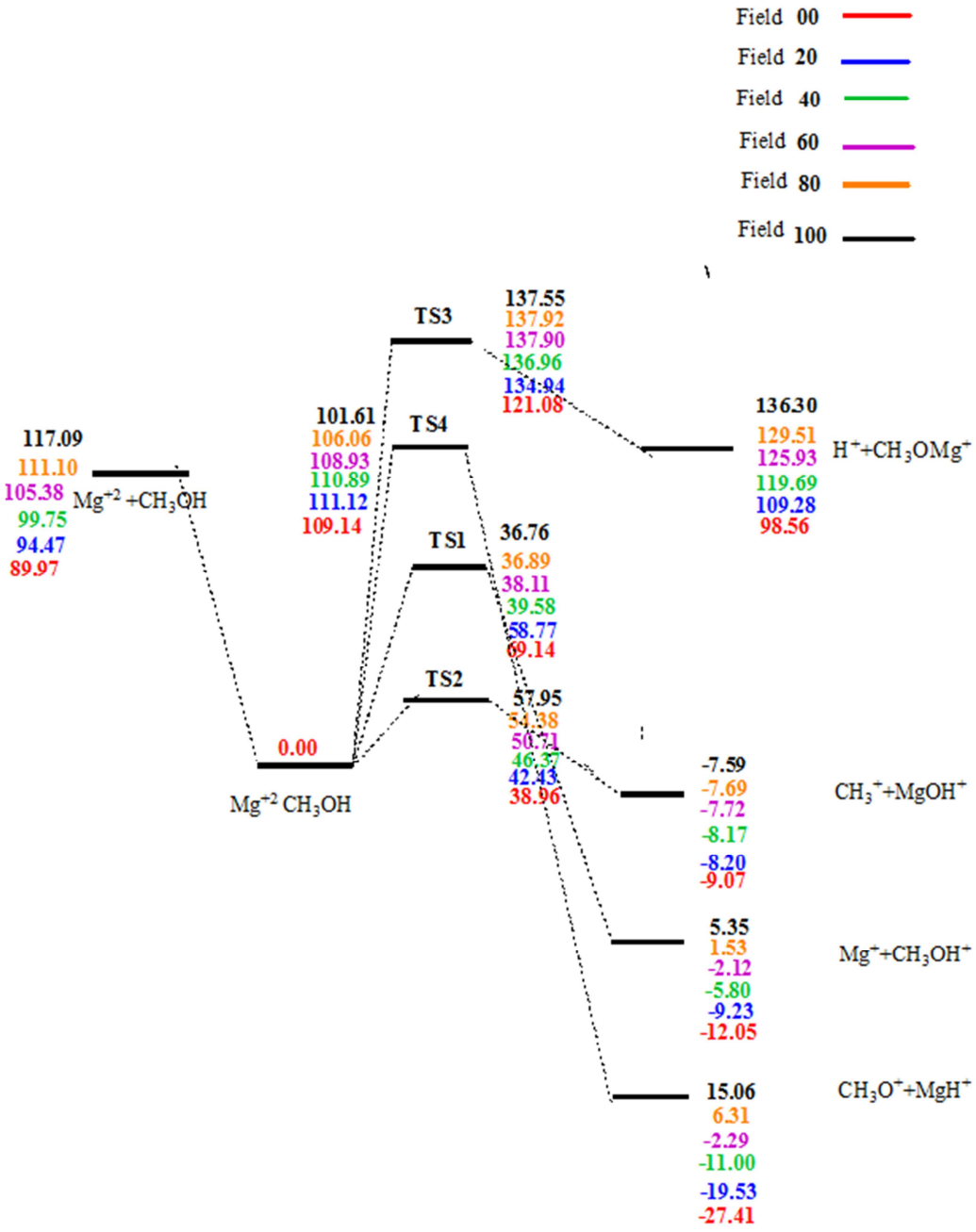

Figure 2. *Energy profile (zero-point corrected relative energies (kcal/mol) for the formation and dissociation of $Mg^{2+}CH_3OH$ at BMK/6- 31 + G (d, p) for increasing the electric fields.*

4. Conclusions

In this paper I have studied thermodynamic and kinetic stability of $Mg^{2+}CH_3OH$ complex under applied electric field to give evidence for the stability of complex under field strength and the possibility of detecting it in the gas phase. This work has been done at the BMK/6-31+G (d) level of theory. The results obtained can be summarized as follows:

1. Based on the thermodynamic behavior for reaction, the $Mg^{2+}CH_3OH$ should not be formed because of the presence of three exothermic channels that means spontaneous dissociation of the complex upon their formation. Moreover the presence of large energy barriers prohibited these dissociation channels and result in kinetically stable mono solvated magnesium dication complex in the gas phase.
2. Systematic and almost uniform variation has been observed for the bond lengths and bond angles of the molecule for various applied Efs.
3. The CH_3OH mono solvated magnesium dication complex is thermodynamically more stable with increasing electric field in the gas phase.
4. The$Mg^{+2}CH_3OH$ complex is kinetically more stable in channels 2 and 4 with increasing electric field in the gas phase.
5. The investigated complex is expected to be detected underappreciated conditions and with increasing the field strength.

References

[1] K. Yamanouchi, Science, Vol. 295, 2002, p. 1659.

[2] P. Sharma, R. K. Vasta, D. K. Maity, S. K. Kulshreshtha, Chem. Phys. Lett, Vol. 382, 2003, p.637.

[3] C.-Y. Wu, Y.-J. Xiong, N. Ji, Y. He, Z. Gao, F. Kong, J. Phys. Chem. A. Vol. 105, 2001, p. 374.

[4] Y.-Q. Wang, J.-Y. Zhu, L. Wang, S.-L. Cong, Int. J. Quant. Chem. Vol. 106, 2006, p. 1138.

[5] R. Itakura, K. Yamanouchi, T. Tanabe, T. Okamoto, F. Kannari, J. Chem. Phys. Vol. 119, 2003, p. 4179.

[6] P. Tzallas et al., Chem. Phys. Lett. Vol. 343, 2001, p. 91.

[7] M. Ueyama, H. Hasegawa, A. Hishikawa, K. Yamanouchi, J. Chem. Phys. Vol. 123, 2005, p. 154305.

[8] S. Shaik, S. P. de Visser, D. Kumar, J. Am. Chem. Soc. Vol. 126, 2004, p. 11746.

[9] Y. C. Choi, C. Pak, K. S. Kim, J. Chem. Phys. Vol. 124, 2006, p. 094308.

[10] H. Kono, Y. Sato, N. Tanaka, T. Jato, K. Nakai, S. Koseki, Y. Fujimura, Chem. Phys. Vol. 304, 2004, p. 203.

[11] T. S. Zyubina, Y. A. Dyakov, S. H. Lin, A. D. Bandrauk, A. M. Mebel, J. Chem. Phys. Vol. 123 2005, p. 134320.

[12] A. M. Mebel, T. S. Zyubina, Y. A. Dyakov, A. D. Bandrauk, S. H. Lin, Int. J. Quantum Chem. Vol. 102, 2005, p. 506.

[13] H. Benedict, H. H. Limbach, M. Wehlan, W. P. Fehlhammer, N. S. Golubev, R. Janoschek, J. Am. Chem. Soc. Vol. 120, 1998, p. 2939.

[14] M. Ramos, I. Alkorta, J. Elguero, N. S. Golubev, G. S. Denisov, H. Benedict, H. H. Limbach, J. Phys. Chem. A. Vol. 101, 1997, p. 9791.

[15] J. G. Sosnicki, M. Langaard, P. E. Hansen, J. Org. Chem. Vol. 72, 2007, p. 4108.

[16] M. Macernis, B. P. Kietis, J. Sulskus, S. H. Lin, M. Hayashi, L. Valkunas, Chem. Phys. Lett. Vol. 466, 2008, p. 223.

[17] B. S. Mallik, A. Chandra, J. Phys. Chem. A, Vol. 112, 2008, p. 13518.

[18] I. Mata, E. Molins, I. Alkorta, E. Espinosa, J. Chem. Phys. Vol. 130, 2009, p. 044104.

[19] Y. Furukawa, K. Hoshina, K. Yamanouchi, H. Nakano. Chem. Phys. Lett. Vol. 414, 2005, p. 117−121.

[20] T. Okino, Y. Furukawa, P. Liu, T. Ichikawa, R. Itakura, K. Hoshina, K. Yamanouchi, H Nakano,. Chem. Phys. Lett. Vol. 419, 2006, p. 223−227.

[21] T. Okino, Y. Furukawa, P. Liu, T. Ichikawa, R. Itakura, K. Hoshina, K. Yamanouchi, H Nakano, Phys. B. Vol. 39, 2006, p. S515−S521.

[22] P. Liu, T. Okino, Y. Furukawa, T. Ichikawa, R. Itakura, K. Hoshina,. K. Yamanouchi, H. Nakano, Chem. Phys. Lett. Vol. 423, 2006, p. 187−191.

[23] T. Okino, Y. Furukawa, P. Liu, T. Ichikawa, R. Itakura, K. Hoshina,.; K. Yamanouchi, H. Nakano, Chem. Phys. Lett Vol. 423, 2006, p. 220−224.

[24] R. Itakura, P. Liu, Y. Furukawa, T. Okino, K. Yamanouchi, H. Nakano. J. Chem. Phys. Vol. 127,.2007, p. 104306.

[25] H. Xu, C. Marceau,. K. Nakai, T. Okino, S.-L Chin, K. Yamanouchi, J. Chem. Phys. Vol. 133, 2010, p. 071103.

[26] Xu, H.; Okino, T.; Kudou, T.; Yamanouchi, K.; Roither, S.; Kitzer, M.; Batuska, A.; Chin, S.-L. Effect of Laser Parameters on Ultrafast Hydrogen Migration in Methanol Studied by Coincidence Momentum Imaging. J. Phys. Chem. A. Vol.116, 2012, p. 2686−2690.

[27] Evelyn J. L. Toledo, Rogério Custodio, Teodorico C. Ramalho, Maria Eugênia Garcia Porto b, Zuy M. Magriotis. Journal of Molecular Structure: THEOCHEM, Vol. 915, 2009, p. 170–177.

[28] E. M. Stuve, Chemical Physics Letters, Vol. 519–520, 2012, p. 1–17.

[29] A. Modal, H. Seenivasan, S. Saurav and A. K Tiwari, Idian journal of chemistry, Vol. 52A, 2013, p. 1056-1060.

[30] H. siu-Feng Lu, F.-Y. Li, Chun-Chin Lin, K. Nagaya, Ito Chao, S. H. Lin, Chemical Physics Letters. Vol. 443, 2007, p. 178–182.

[31] S. Azam, A. H. Reshak, Int. J. Electrochem. Sci., Vol. 8, 2013, p. 10359.

[32] D. Rai, A. D. Kulkarni, S. P. Gejji, L. J. Bartolotti, R. K. Pathak, Journal of chemical physics, Vol. 138(4), 2013, p.044304.

[33] W J, A. Hehre, Inc. Irvine, CA, 2003.

[34] Jensen F, Introduction to Computational Chemistry, John Wiley & Sons Ltd., England, 2007.

[35] R. F. W. Bader Atoms in molecules - A quantum theory, Clarendon Press Oxford, 1990; Kryachko E S, Ludena E, Energy Density functional theory of atoms of many electron system: Academic Newyork, 1990.

[36] J. M. Seminario, Elesvier New York, 1996.

[37] M. J. Frisch, G. W. Trucks, H. B. Schlegel, G. E. Scuseria, M. A. Robb, J. R. Cheeseman, G. Scalmani, V. Barone, B. Mennucci, G. A. Petersson, H. Nakatsuji, M. Caricato, X. Li, H. P. Hratchian, A. F. Izmaylov, J. Bloino, G. Zheng, J. L. Sonnenberg, M. Hada, M. Ehara, K. Toyota, R. Fukuda, J. Hasegawa, M. Ishida, T. Nakajima, Y. Honda, O. Kitao, H. Nakai, T. Vreven, J. A. Montgomery, Jr., J. E. Peralta, F. Ogliaro, M. Bearpark, J. J. Heyd, E. Brothers, K. N. Kudin, V. N. Staroverov, R. Kobayashi, J. Normand, K. Raghavachari, A. Rendell, J. C. Burant, S. S. Iyengar, J. Tomasi, M. Cossi, N. Rega, J. M. Millam, M. Klene, J. E. Knox, J. B. Cross, V. Bakken, C. Adamo, J. Jaramillo, R. Gomperts, R. E. Stratmann, O. Yazyev, A. J. Austin, R. Cammi, C. Pomelli, J. W. Ochterski, R. L. Martin, K. Morokuma, V. G. Zakrzewski, G. A. Voth, P. Salvador, J. J. Dannenberg, S. Dapprich, A. D. Daniels, O. Farkas, J. B. Foresman, J. V. Ortiz, J. Cioslowski, and D. J. Fox, Gaussian, Inc., Wallingford CT, 2009.

[38] A. D. Boese, J. M. L. Martin, Chem. Phys. Vol. 121, 2004, p. 3405-*3416.*

[39] G. A. Zhurko, D. A. Zhurko, ChemCraft version 1.8.

[40] A. E. Reed, R. B. Weinstock, F. A. Weinhold,. J. Chem. Phys. Vol., 83, 1985, p. 735-746.

[41] M. Ichihashi, C. A. Corbett, T. Hanmura, J. M. Lisy, T. Kondow, J. Phys. Chem. A, Vol. 109, 2005, p. 7872.

[42] A. M. El-Nahas, S. H. El-Demerdash, S. E. El-Shereefy, International Journal of Mass Spectrometry, Vol. 263, 2007, p. 267–275

[43] T. Ljjima, J. Mol. Struct. Vol. 212, 1989, p. 137.

[44] D. Farmanzadeh, Z. Ashtiani,, Struct. Chem. Vol. 21, 2010, p. 691.

[45] J. Mazurkiewicz, P. Tomasik, Natural Science, Vol. 4, 2012, p. 276.

[46] B. Kirtman, B. Champagne, D. M. J. Bishop, J. Am. Chem. Soc. Vol. 122, 2002, p. 8007.